DUST RELATIVE VELOCITIES IN THE VICINITY OF A GAP-OPENING JUPITER-MASS PLANET. Augusto Carballido, Lorin S. Matthews, and Truell W. Hyde. Center for Astrophysics, Space Physics and Engineering Research, Baylor University, Waco, TX 76798, USA

Introduction: The role of dust in interpreting images of protoplanetary disks with gaps cannot be overstated [1]. Numerical investigations of the dynamics of dust particles in the neighborhood of a gap-opening planet reveal that they tend to concentrate at gap edges, for planet masses between ~ $0.03M_J$ and $5M_J$, with M_J the mass of Jupiter [2,3,4]. One aspect of the evolution of dust in the vicinity of a gap-opening planet that has not been considered is the internal structure of solid aggregates. The porosity of dust particles affects their aerodynamic coupling to the disk gas. Their structure can also affect the ionization state of the protoplanetary disk, and thus render the disk gas stable to the magneto-rotational instability, or MRI [5]. Electric charges lead to larger, more massive and more porous aggregates than in the case of neutral coagulation [7]. To better characterize the spatial distribution of dust grain sizes and porosities around a Jupiter-mass planet, we combine a numerical model of a protoplanetary disk subject to MRI turbulence with a Monte Carlo dust coagulation algorithm. In the interest of specificity, we use our models to invoke a scenario in which Jupiter underwent migration within the primitive solar nebula, the so-called Grand Tack hypothesis [8]. In this first stage of our investigation, we calculate the relative velocities between dust particles and allow only sticking plus compaction, and we defer the inclusion of other collisional outcomes to a future analysis.

Method: *Disk model*. We use a magnetohydrodynamic (MHD) protoplanetary disk model in the local shearing box approximation [9], in which the MHD equations are solved in a rectangular coordinate system that corotates with the disk at a fiducial orbital radius R_0, with angular frequency Ω_0. In this system, the *x* axis is oriented along the radial direction, the *y* axis along the azimuthal direction, and the *z* axis is parallel to the disk's angular momentum vector. The MHD solver used is the Athena code [10]. The numerical setup is similar to that of [11]: the local, 3D disk model is isothermal, and does not include vertical stratification of the gas density. The box dimensions are $16H \times 16H \times H$, where H is the disk scale height. We use a numerical resolution of 64 grid cells per H. The initial magnetic field strength is given by the plasma beta, β=400, and the initial field configuration corresponds to a non-zero net vertical magnetic flux. Ideal MHD conditions are assumed.

To model the gravitational effect of a planet on the surrounding disk gas, we place a cylindrical potential at the center of the box, with axis coincident with the box's vertical axis [11]. We give the planet a mass $M_p = 1\ M_J$ and choose its orbital radius to be $R_p = 3$ AU, consistent with the Grand Tack scenario [8].

We run this high-resolution setup for 51 orbits (265 yr at 3 AU in the Minimum Mass Solar Nebula), and use the resulting data from the last 12 orbits, after the gas flow reaches an approximate steady state.

Collisional velocities. Our treatment of dust coagulation follows the implementation of [12]. We calculate the relative speed Δv_{ij} between two particles i and j from two contributions: Brownian motion and turbulence. The latter contribution, given in [13], depends on the gas turbulent velocity v_g, the gas turbulent viscosity ν_T, and the particle Stokes numbers $St_{i,j}$, which parameterize the aerodynamic coupling of solids to the gas. The Stokes numbers, in turn, depend on the gas density, ρ_g.

We obtain the values of v_g, ν_T, and ρ_g from the MHD simulation of the gap-opening process. These values are taken from four different regions, labeled R1 through R4, in the vicinity of the planet, as shown in Fig. 1, which portrays the system at the end of the simulation. The gas surface density is shown. The gap opened by the planet is clearly defined. The gas variables are averaged inside each region, and are then passed on to the dust algorithm. The particles do not have position coordinates associated with them.

Results: Figure 2 shows radial profiles of several quantities associated with the MHD flow. These quantities have been averaged over time (the last 12 orbits of the simulation) and over the *y* and *z* directions. The vertical gray bars mark the radial position of the reference regions. In Fig. 2a, the gas density, normalized by its initial value, drops by a factor of ~ 10 inside the gap opened by the planet with respect to the surrounding gas. Panel c shows a corresponding factor-of-8 drop in the Maxwell stress, which is the main contributor to the turbulent viscosity in accretion disks [9]. Figure 2b shows the turbulent gas velocity in units of the gas sound speed. Finally, Fig. 2d reveals that the mean vertical magnetic field has two maxima at either side of the planet's radial position, close to the gap edges. This is in contrast to the centrally-peaked profile of $\langle B_z \rangle_{yz}$ measured by [11], for a lower planet mass of ~ $0.15M_J$.

The relative speeds of dust particles involved in each collision are shown in Fig. 3, for each of the regions of Fig. 1. The highest relative speeds are generated in

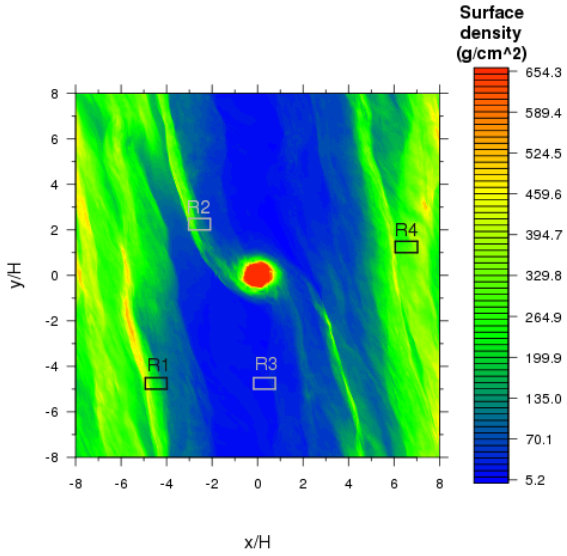

Figure 1: Gas surface density at the end of the MHD simulation. The rectangles labeled R1 through R4 mark the locations from which gas velocities, densities and stresses are fed to the dust particle coagulation code.

region R3, where the turbulent gas velocity has the highest magnitudes.

Discussion: At the relative speeds calculated inside the planetary-induced gap (in the range ~ 50 – 600 cm/s), relative kinetic energies exceed the minimum energy required for restructuring of dust aggregates. Preliminary analyses show that inside the gap (R3) aggregate porosities would achieve their lowest values (~ 48%), if the initial particle size distribution is monodisperse, with an initial monomer radius of 1 μm. Aggregate collisions in this region will also result in fragmentation, which will be included in a later model. In the high-gas-density regions outside the gap (e.g., R1 and R4), the relative velocities are much lower leading to gentle collisions. In R4 in particular porosities could reach extremely high values of ~ 98%.

References: [1] Gonzalez J. –F. et al. (2015) *MNRAS, 454,* L36. [2] Fouchet L. et al. (2007) *A&A, 474,* 1037. [3] Zhu Z. et al. (2014) *ApJ,* 785,122. [4] Picogna G. and Kley W. (2015) *A&A, 584, 110.* [5] Balbus S. A. and Hawley J. F. (1991) *ApJ, 376, 214.* [6] Lubow S. H. et al. (1999), *ApJ, 526, 1001.* [7] Matthews L. S. et al. (2012) *ApJ, 744, 8.* [8] Walsh K. J. et al. (2011) *Nature, 475, 206.* [9] Hawley J. F. et al. (1995) *ApJ, 440, 742.* [10] Stone J. M. et al. (2008) *ApJS, 178, 137.* [11] Zhu Z. et al. (2013) *ApJ, 768, 143.* [12] Ormel C. W. et al. (2007) *A&A, 461, 215.* [13] Ormel C. W. et al. (2008) *ApJ, 679, 1588.*

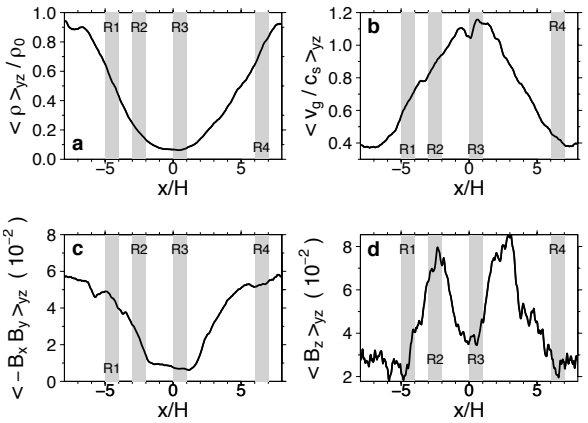

*Figure 2: Radial profiles of **(a)** gas density normalized by its initial value, **(b)** gas turbulent velocity in units of the sound speed, **(c)** x-y component of magnetic stress tensor, and **(d)** vertical component of magnetic field. Vertical gray bars denote the radial position of the reference regions in Fig. 1.*

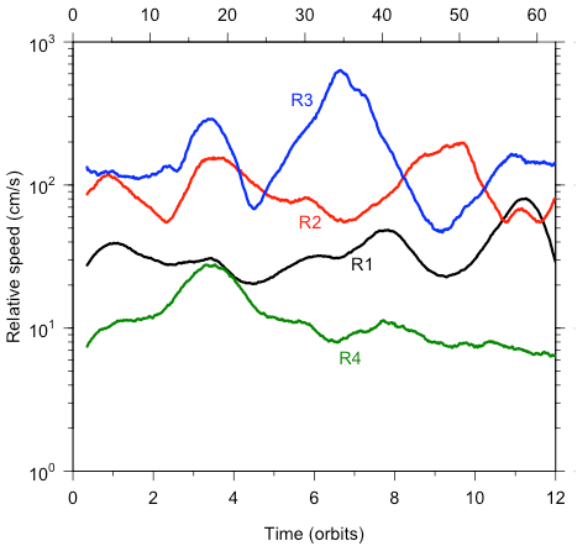

Figure 3: Simple moving average (SMA) of relative speed between the two particles involved in each collision. The SMA is taken every 0.35 orbits. Each curve color corresponds to a region Rn (n=1,...,4) of Fig. 1.